Carbohydrate Polymers 121 (2015) 56–63

Contents lists available at ScienceDirect

Carbohydrate Polymers

journal homepage: www.elsevier.com/locate/carbpol

Lysozyme depolymerization of photo-activated chitosan adhesive films

Damia Mawad[a], Charles Warren[b], Mathew Barton[c], David Mahns[c], John Morley[c], Binh T.T. Pham[d], Nguyen T.H. Pham[d], Sindy Kueh[c], Antonio Lauto[c,e,*]

[a] Department of Materials, Department of Bioengineering and Institute for Biomedical Engineering, Imperial College London, Exhibition Road, London SW7 2AZ, UK
[b] School of Biological Sciences, The University of Sydney, Sydney 2006, NSW, Australia
[c] School of Medicine, University of Western Sydney, Locked Bag 1797, Penrith 2751, NSW, Australia
[d] Key Centre for Polymers and Colloids, School of Chemistry, University of Sydney, Sydney 2006, NSW, Australia
[e] Biomedical Engineering & Neuroscience (BENS) Research Group, The MARCS Institute, University of Western Sydney, Locked Bag 1797, Penrith 2751, NSW, Australia

ARTICLE INFO

Article history:
Received 11 October 2014
Received in revised form 8 December 2014
Accepted 10 December 2014
Available online 31 December 2014

Keywords:
Lysozyme
Laser
Capillary electrophoresis
Mass spectroscopy

ABSTRACT

Effective tissue bioadhesion of rose bengal–chitosan films can be achieved by photoactivation using a green laser. In this study, lysozyme was incorporated in these films to enhance the rate of depolymerization and assess the laser impact on lysozyme. The lysozyme loaded films exhibited a 21% mass loss after 4 weeks implantation in rats while control films (without lysozyme) had only 7% mass loss. Capillary electrophoresis–mass spectroscopy showed that chitosan degraded into monomers and oligomers of glucosamine and *N*-acetyl-glucosamine. Irradiation with laser did not affect the depolymerization of adhesive by lysozyme suggesting that the inclusion of lysozyme in the bioadhesive is a viable technique for tailoring the depolymerization.

1. Introduction

Investigating the degradation profiles of a biomaterial is essential when designing an implant since the degradation rate will have direct influence on the performance of the medical device including its stability, mechanical properties, host response and tissue regeneration (Sionkowska, 2011; Azevedo & Reis, 2007). As part of our on-going research to develop a chitosan based bioadhesive for nerve and tissue repair (Lauto et al., 2010, 2012; Barton et al., 2013a,b), we investigate the *in vitro* and *in vivo* depolymerization rate of chitosan adhesives by incorporating lysozyme within the films.

Chitosan, a polysaccharide that is the deacetylated form of chitin, is biocompatible and consequently widely used in tissue engineering scaffolds (Aranaz et al., 2009; Muzzarelli, 2009; Kim et al., 2008). Although classified as a biodegradable biopolymer that can be enzymatically hydrolysed by lysozyme, its depolymerization rate varies widely depending on its degree of deacetylation or its molecular weight (Kean & Thanou, 2010). Additionally, the depolymerization rate of chitosan has been shown to differ as function of the fabrication technique of the final designed product, *i.e.* a hydrogel (Obara et al., 2003), film (Zhao, Wang, Zhao, & Pan, 2002), fiber (Kim, Tator, & Schoichet, 2011) or microsphere (Mi, Tan, Liang, & Sung, 2002). Hence, it is critical to assess the depolymerization rate of chitosan bioadhesives intended for use as new medical implants to replace sutures. Unmodified chitosan films, containing the dye rose bengal (RB), have been shown to become a strong tissue adhesive when activated by green light (bonding strength ~15 kPa), and to repair *in vivo* peripheral nerves without sutures (Barton et al., 2012, 2013a,b, 2014). The mechanism of adhesion is not clear yet, although it was observed that rose bengal diffuses from the adhesive towards the tissue interface; this in turn may facilitate the crosslinking between chitosan and collagen molecules upon green light photoactivation, which generates singlet oxygen ($^1O_2$) (Verter et al., 2011; Kochevar & Redmond, 2000). Chitosan scaffolds and films have also been reported to depolymerize over a long period of time (>3 months) (Costa-Pinto et al., 2014), prompting the need to accelerate or better control this biochemical process. In this study we therefore attempted to manipulate the depolymerization rate by integrating lysozyme within the bioadhesives. Since the adhesion of RB–chitosan films is triggered by photo-activation, it is

* Corresponding author at: University Western Sydney, School of Medicine, Locked Bag 1797, Macarthur, Penrith 2751, NSW, Australia. Tel.: +61 450313689.
E-mail address: a.lauto@uws.edu.au (A. Lauto).

http://dx.doi.org/10.1016/j.carbpol.2014.12.008
0144-8617/

imperative to establish that lysozyme incorporated within retains its activity after laser irradiation. This could be shown by assessing the *in vitro* depolymerization rate of these films incubated in physiological conditions (pH = 7.4, 37 °C) as well as by determining the depolymerization products resulting from the films and showing that they are of similar size and structure to what is commonly reported for the enzymatic depolymerization of chitosan. For this purpose, capillary electrophoresis–mass spectrometry (CE–MS) is a powerful technique that could be employed to determine the mass and nature of the depolymerized products. CE–MS is proven to be a viable technique for the separation of both charged and uncharged compounds as well as the separation of oligomers and polyelectrolytes (Cottet & Gareil, 2000; Mnatsakanyan et al., 2013).

The aim of this study was to investigate whether the depolymerization rate of chitosan based bioadhesives could be tailored by adding lysozyme during their fabrication. Of significance, we have established that irradiating the lysozyme-loaded films with the green laser does not affect the enzyme activity. *In vitro* depolymerization studies were carried out by incubating the films in phosphate buffer solution (PBS) at 37 °C and their weight was monitored over predetermined time points. *In vivo* studies were carried out by subcutaneously implanting the films in the right dorsal scapular region of rats. Gravimetric analysis was applied to assess the depolymerization mass loss from both *in vitro* and *in vivo* implanted chitosan adhesives. To confirm the occurrence of enzymatic depolymerization, CE–MS was used to determine the presence/absence of monomers and oligomers of glucosamine and *N*-acetyl-glucosamine. The morphology of the depolymerized films was investigated using scanning electron microscopy (SEM).

2. Materials and methods

2.1. Materials

Chitosan (~590 CPs medium molecular weight (MMW), ~13% degree of acetylation), lysozyme from chicken egg white and all other chemicals were purchased from Sigma and used as received.

2.2. Fabrication of lysozyme loaded chitosan adhesives

Chitosan films loaded with different amounts of lysozyme (0.5, 1, 3 and 5 mg/mL) were prepared and their depolymerization rate was assessed. For instance, chitosan films loaded with 1 mg/mL of lysozyme were prepared as follows: 0.85 g of chitosan was added to 2% (v/v) acetic acid aqueous solution (40 mL) and left stirring for 1 week to completely dissolve. Lysozyme (50 mg) was dissolved in 2% (v/v) acetic acid aqueous solution (10 mL) and then added to the chitosan solution to prepare a final concentration of 1 mg/mL lysozyme and 1.7% (wt/v) chitosan. The lysozyme–chitosan solution was stirred for 30 min followed by centrifugation at 4000 rpm for 20 min at 4 °C. The supernatant was collected and the solid pellet discarded. The supernatant was spread evenly (2.4 mL over 16 cm^2) over a sterile and dry perspex plate. The solutions were allowed to dry shielded from light under clean conditions and atmospheric pressure, until they became insoluble in water (~3 weeks at 4 °C) (Lauto et al., 2012).

2.2.1. Laser irradiation

To ensure that the laser does not affect the depolymerization activity of the lysozyme, rose bengal–chitosan (RB–chitosan) films containing 1 mg/mL lysozyme were prepared. The RB–chitosan solution was prepared as follows: chitosan (0.85 g) and RB (0.007 g) were added to 2% (v/v) acetic acid aqueous solution (40 mL) and left stirring for 2 weeks to completely dissolve the rose bengal. Lysozyme (50 mg) was dissolved in 2% (v/v) acetic acid aqueous solution (10 mL) and then added to the RB–chitosan solution to prepare a final concentration of 1 mg/mL lysozyme, 1.7% (wt/v) chitosan and 0.014% (wt/v) RB; films were then prepared following the method described above (Lauto et al., 2012). The RB–chitosan films were irradiated by a solid-state diode-pumped laser (λ = 532 nm, CNI Lasers, China), which was coupled to a multimode optical fiber with a core diameter of 200 μm and numerical aperture of 0.22. The Fluence and Irradiance applied over the adhesive were 120 ± 10 J/cm^2 and ~0.9 W/cm^2, respectively, as detailed in previous publications (Lauto et al., 2010, 2012; Barton et al., 2013a,b). Results were analysed using two-way ANOVA and Bonferroni post-test at a significance level of 5%.

2.3. In vitro degradation of lysozyme loaded chitosan adhesives

The dried films loaded with lysozyme were cut to a standard size (area = 16.0 ± 0.8 cm^2, thickness 24 ± 3 μm), lyophilized, weighed (m_i) and then transferred to permeable tea bags. The samples were sterilized with 70% (v/v) of ethanol aqueous solution and left to dry at room temperature in a sterilized hood for 1 h. Films were then incubated in 50 mL PBS (pH 7.4) at 37 °C. At different time points, three tea bags (n = 3) were removed from the degrading medium, lyophilized, and reweighed to get the dry weight of the depolymerized films (m_d). The % mass loss was calculated as follows:

$$\%\ \text{mass loss} = \frac{(m_i - m_d)}{m_i} \times 100 \quad (1)$$

2.4. Capillary electrophoresis and mass spectroscopy (CE–MS)

2.4.1. Sample preparation

The *in vitro* depolymerization of RB–chitosan films (~1 × 1 cm, containing 1 mg/mL lysozyme) was also investigated using CE–MS. Three films were laser-irradiated while three others were not, before being sterilized with 75% alcohol and air dried; the films were then incubated in sterile vials containing PBS (3 mL) and placed in an incubator at 37 °C for 1 week before their supernatant was analysed by CE–MS. In a separate instance, RB–chitosan films (1 × 1 cm) were prepared without incorporating lysozyme and incubated in sterile vials containing PBS (3 mL) and lysozyme (1 mg/mL). These films underwent the same procedure described above, before being analysed by CE–MS. Other RB–chitosan adhesive films (laser-irradiated and non-irradiated) were also incubated in PBS solutions without lysozyme, to serve as controls. Three samples were prepared and analysed for each experimental and control group (n = 3).

2.4.2. CE–MS procedures

Capillary electrophoresis–mass spectrometry was used for untargeted profiling of depolymerization products of chitosan films, which were immersed in lysozyme solutions. The CE–MS procedure was essentially described previously (Warren, 2013); CE–MS was performed with a capillary electrophoresis system (P/ACE MDQ, Beckman-Coulter, Fullerton, CA, USA) equipped with a bare fused silica capillary (50 μm i.d. × 100 cm long) interfaced *via* a co-axial sheath-flow sprayer (G1607A, Agilent, Waldbronn, Germany) to an ion trap mass spectrometer (AmaZon SL, Bruker Daltonics, Bremen, Germany). Sheath liquid of 50% (v/v) methanol with 0.1% (v/v) formic acid was delivered at 4 μL/min. Electrospray ionizaton (ESI) was achieved under the following conditions: dry gas N_2 (4 L/min) at 200 °C, nebulizer 6 psi, electrospray in positive mode at −4.5 kV. Ultra high purity helium (99.999%, BOC, Sydney, NSW, Australia) was used as the ion trap damping gas. To obtain a broad coverage of potential molecular weights and ensure high sensitivity, samples were analysed first with a scan range of 50–250 m/z to detect monomers and small oligomers, and subsequently with a broader scan range to detect larger oligomers

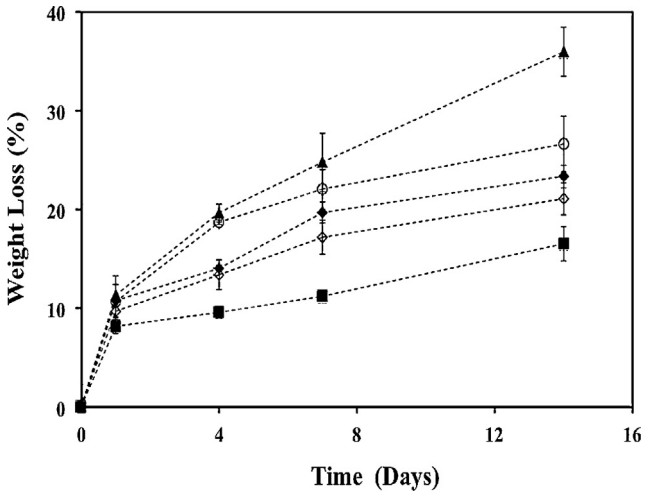

Fig. 1. *In vitro* depolymerization: average % mass loss of chitosan adhesives loaded with (■) 0.5 mg/mL, (◊) RB + 1 mg/mL + laser, (♦) 1 mg/mL, (○)3 mg/mL and (▲) 5 mg/mL lysozyme. The laser irradiation did not affect the adhesive depolymerization. The lines are to guide the eye.

and polymers. Preliminary experiments with scan ranges up to 2200 *m*/*z* established there were few ions greater than 1250 *m*/*z*, and thus a scan range of 150–1500 *m*/*z* was used. Ion transmission was optimized using smart parameter setting with a target mass of 100 *m*/*z* for 50–250 Da scans and a target of 750 *m*/*z* for 150–1500 *m*/*z* scans. Samples containing internal standard (0.4 μg/mL methionine sulfone) were injected at 3 psi for 30 s and separated with an electrolyte of 1 M formic acid under 30 kV positive polarity. The mass spectrometer scanned in enhanced resolution mode (8100 Da/s) with data recorded as the average of five scans (50–250 Da scan range) or three scans (150–1500 Da scan range). Between runs the capillary was flushed with electrolyte for 10 min (50 psi).

2.4.3. CE–MS compound ID

The monomeric compounds glucosamine and *N*-acetyl-glucosamine were identified in 50–250 *m*/*z* scans based on comparison of migration times and $[M+H]^+$ with authentic standards run under the same conditions on the same instrument. For identification of oligomeric and polymeric compounds detected in 150–1500 *m*/*z* scans, MS/MS spectra were obtained by re-analyzing samples under the same electrophoretic conditions. Auto MS^n data acquisition was performed with three MS/MS precursors per MS, active exclusion after two spectra, including after 0.3 min, isolation width of 1.5 *m*/*z*, fragmentation amplitude of 0.8 V modulated by SmartFrag from 60 to 200% with 40 ms activation time.

2.5. Animal model

The animal care and ethics committee at the University of Western Sydney approved all animal experiments in this study (A8900). Forty-eight female Long Evans rats (UWS animal house, Campbelltown, NSW), weighing 190–220 g were aneasthetized using 2% isofluorane in 100% oxygen using a standard anaesthetic machine. Under sterile conditions, a 30 mm parasagittal skin incision was made upon the right dorsal scapular region using an Olympus operating microscope (1–40×). The skin was reflected from the underlying subcutaneous tissue on each side of the incision by a width of 10 mm. Each animal was assigned to one of the two experimental groups and over two of the post-operative periods (1 and 4 weeks). Postoperatively, animals were housed in the UWS School of Medicine animal facility with unlimited access to water and rat chow.

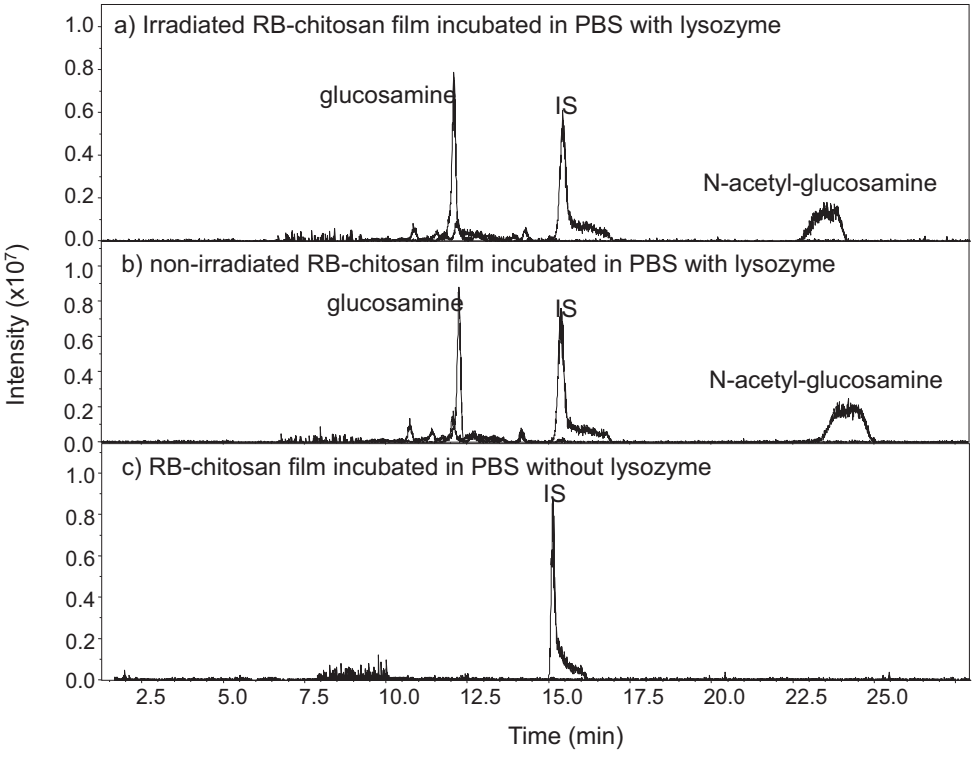

Fig. 2. CE–MS (50–250 Da scan range) of monomeric compounds liberated from RBchitosan films that were (a) irradiated then incubated with PBS + lysozyme, (b) not irradiated then incubated with PBS + lysozyme, or (c) not irradiated and then incubated in PBS without lysozyme. Data are extracted ion electropherograms for masses corresponding to protonated glucosamine, *N*-acetyl-glucosamine and the internal standard (IS). Glucosamine and *N*-acetyl-glucosamine were also detected in RB–chitosan films that contained lysozyme (data not shown).

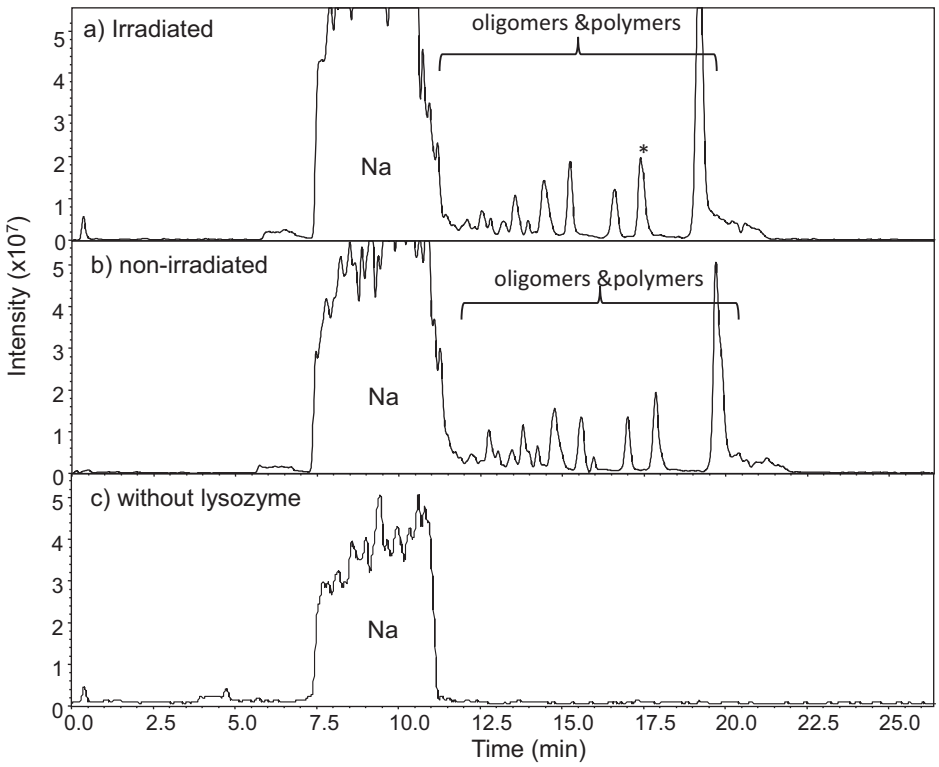

Fig. 3. CE–MS (150–1500 Da scan range) of compounds liberated from RB–chitosan films that were (a) irradiated then incubated with PBS + lysozyme, (b) not irradiated then incubated with PBS + lysozyme, or (c) not irradiated and then incubated in PBS without lysozyme. Shown is a basepeak electropherogram (the intensity of the most intense peak at every point in the analysis). From 7 to 11 min there is a large peak due to sodium from the PBS buffer, while from 12 min onwards there are a series of peaks originating from organic compounds. The asterisk indicates one of many peaks that was analysed by MS/MS (see Fig. 5).

2.5.1. Group 1, lysozyme loaded rose adhesive (n = 24)

Following skin reflection, a RB–chitosan film containing 1 mg/mL lysozyme with dimensions ~25 × 15 mm was weighed then sterilized (70% ethanol) and washed with sterile saline solution before being positioned on top of the exposed subcutaneous tissue with microforceps. The films were either laser-irradiated ($n = 12$) or non-irradiated ($n = 12$) before being implanted in animals. The lysozyme concentration of 1 mg/mL was selected as it is within the physiological range, being typically found in human tears (Temel, Kazokoglu, & Taga, 1991). The wound was closed using surgical staples and treated with self-mutilation deterrent antiseptic solution. Animals were sacrificed one week ($n = 6$) or four weeks ($n = 6$) after the operation to assess: (a) the change in the dry weight of the adhesive, and b) the adhesive's surface topography by scanning electron microscopy (SEM) as will be described.

2.5.2. Group 2, rose adhesive (n = 24)

In this group, the same procedure described in Group 1 was adopted with the exception of using RB-adhesive without lysozyme.

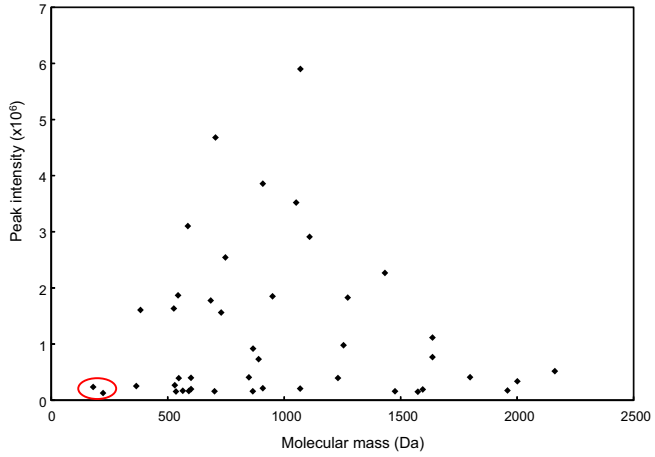

Fig. 4. Mass distribution of depolymerization products detected by CE–MS of adhesive incubated with lysozyme (Figs. 2a and 3a). To determine the mass of compounds, m/z data from CE–MS were deconvoluted. Glucosamine and *N*-acetylglucosamine are indicted by a red circle. (For interpretation of the references to color in this figure legend, the reader is referred to the web version of this article.)

2.6. In vivo degradation of the adhesives

The surgical site for both group 1 and 2 was reopened after their respective weeks; following adhesive removal from *in situ*, five films from each experimental group were individually washed in normal saline (to remove unwanted tissue/blood) placed into a vacuum pump crucible, sealed and immersed into liquid nitrogen for 1 min (to freeze adhesive). The crucible was then attached to the freeze dryer (CHRIST ALPHA1-2 LDPlus, fisher bioblock scientific, France) and run at −76 °C with 0.0010 mbar of vacuum for 8 h. The dried adhesives were then weighed and the mass loss calculated according to Eq. (1) as described in the *in vitro* depolymerization protocol.

2.7. Scanning electron microscopy (SEM)

The surface topography of each experimental group pre and post laser irradiation was imaged on a scanning electron microscope (Zeiss ULTRA Plus) using In-lens secondary electron detector. A piece of dry film (50 × 50 mm) from each group was mounted on a carbon tape coated stub. The film surface was examined without an additional coating to avoid introduction of artefacts onto the

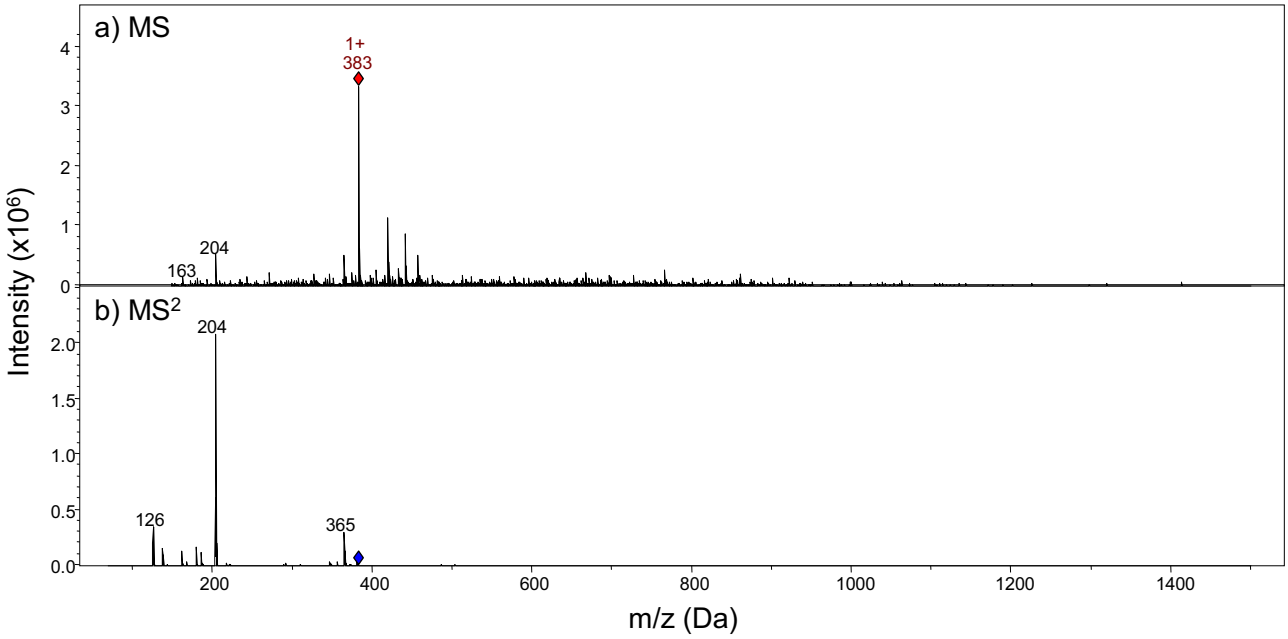

Fig. 5. MS_1 spectra (a) and MS_2 spectra (b) of the peak migrating at 18 min in Fig. 3. The sample was injected and separated as described for Fig. 3, but with autoMS_n being used to obtain MS/MS spectra. AutoMS_n data acquisition was performed with three MS/MS precursors per MS, active exclusion after two spectra, include after 0.3 min, isolation width of 1.5 *m/z*, fragmentation amplitude of 0.8 V modulated by SmartFrag from 60 to 200% with 40 ms activation time. The compound was putatively identified as Hex–HexNAc.

surface morphology. To obtain surface contrast, a low acceleration voltage of 1 kV was applied to minimize electron penetration.

3. Results

3.1. In vitro degradation of lysozyme-integrated adhesives

In vitro degradation studies were conducted on chitosan adhesive films that were loaded with various concentrations of lysozyme ($n = 3$ for each concentration and time point); upon incubation in PBS, lysozyme is expected to leach out and eventually causes the depolymerization of the films. Fig. 1 shows the mass loss profile of the films over a period of two weeks. The total % mass loss varied from ~17% to ~36% as the concentration of lysozyme in the films increased from 0.5 to 5 mg/mL respectively. No significant depolymerization was detected in chitosan films that did not contain the enzyme. The depolymerization increased significantly at day-7 with respect to day-1 (Two-way ANOVA, Bonferroni post-test, $p < 0.01$) for all types of adhesives except for the 0.5 mg/mL adhesive ($p > 0.05$). At day 14 all types of adhesives presented significant mass loss in comparison to day-1 (two-way ANOVA, Bonferroni post-test, $p < 0.01$).

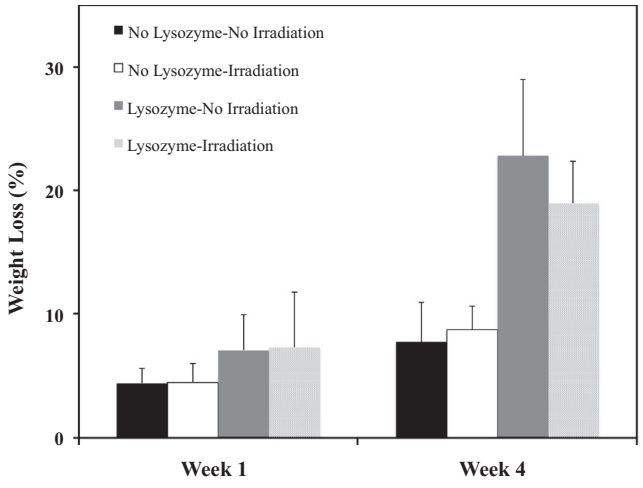

Fig. 6. *In vivo* depolymerization: average % mass loss for chitosan adhesives with and without lysozyme. The adhesive films loaded with lysozyme exhibited a significantly higher mass loss than the adhesive without enzyme after 4 weeks. The laser irradiation did not affect the adhesive break down at any time point.

To ensure the laser did not deactivate the enzyme, RB–chitosan adhesives loaded with lysozyme at the concentration of 1 mg/mL were irradiated before launching the depolymerization study. As shown in Fig. 1, there was no significant difference in mass loss at any time points between the RB irradiated films and the non-irradiated films that were loaded with the same enzyme concentration (two-way ANOVA, Bonferroni post-test, $p > 0.05$). This outcome suggests that the laser had no effect on the depolymerization activity of lysozyme inside the chitosan films. The enzyme depolymerization activity continued for two weeks in our study although lysozyme half-life is ~16 h in physiological conditions (Rogers & Rechsteiner, 1988; Azevedo & Reis, 2007).

3.2. Capillary electrophoresis–mass spectroscopy

The supernatant of the (irradiated and non-irradiated) RB–chitosan films incubated in lysozyme + PBS contained large amounts of glucosamine and *N*-acetyl-glucosamine (Fig. 2a and b) and oligomers (Fig. 3a and b). There was similar liberation of large amounts of glucosamine and *N*-acetyl-glucosamine and oligomers when lysozyme was directly incorporated into RB–chitosan films (irradiated and non-irradiated) and then incubated in PBS (data not shown). None of glucosamine, *N*-acetyl-glucosamine, or oligomers were detected in samples in which films were incubated without lysozyme (either directly incorporated into the film or as a component of the PBS incubation medium; Figs. 2c and 3c).

Mass spectrometry permitted partial characterization of the oligomers, which were liberated from RB–chitosan films that contained lysozyme or were incubated in lysozyme. In addition to

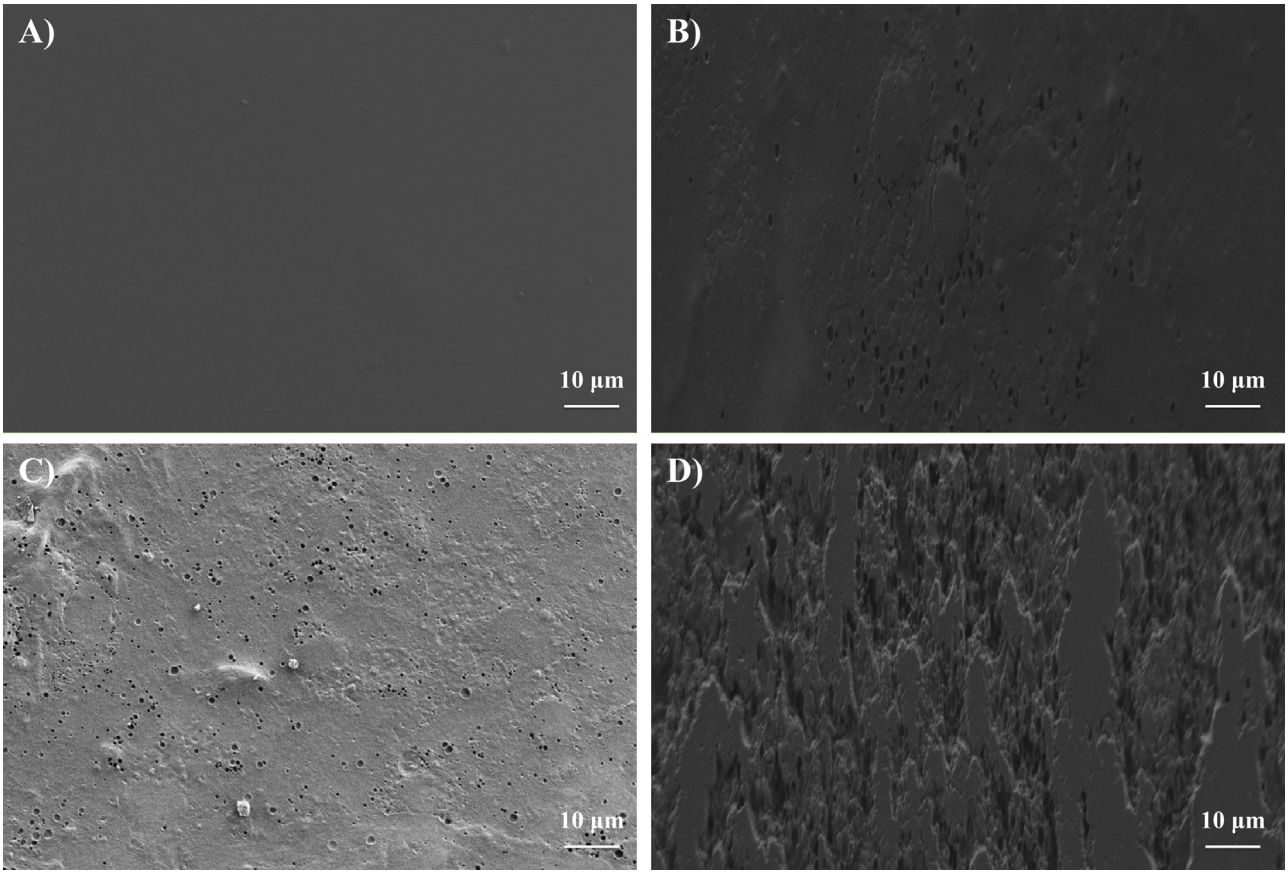

Fig. 7. SEM images of non-irradiated chitosan adhesive (A) containing no lysozyme at fabrication; (B) containing no lysozyme after 4 weeks *in vivo* implantation; (C) containing 1 mg/mL lysozyme after 1 week *in vivo* implantation; (D) containing 1 mg/mL lysozyme after 4 weeks *in vivo* implantation. The irradiated adhesives show similar surface patterns over a 4 weeks period.

the approximately 10 major peaks of oligomers visible in the basepeak electropherogram (Fig. 3a and b), there were at least another one hundred peaks present at lower abundance. Some oligomers were detected as singly charged ions $[M+H]^+$ whereas others were detected as multiply charged ions $[M+nH]^{n+}$ where n represents 2–5 hydrogen cations. To determine the mass of compounds, *m/z* data from CE–MS were deconvoluted and after taking account of multiple charging, the detected molecules were found to have masses spanning from 180 Da (protonated glucosamine) and 222 Da (protonated *N*-acetyl-glucosamine) up to approximately 2200 Da (Fig. 4).

MS/MS indicated that the putative oligomer peaks fragmented to produce marker ions characteristic of hexosamines and/or *N*-acetyl-hexosamines. For example, manual inspection of the approximately 100 peaks isolated and fragmented by autoMS^n indicated that peaks fragmented to produce MS^2 ions with masses of 162, 180 and 204 Da that are characteristic of compounds containing hexosamine and *N*-acetyl-hexosamine (Fig. 5). These findings indicate that lysozyme leads to extensive depolymerization of chitosan into monomers and oligomers of glucosamine and *N*-acetyl-glucosamine.

3.3. Post-operative gross findings

All animals survived the surgical procedure and were in good health until the end of the respective experiments. No infections or complications were observed.

3.4. In vivo degradation of lysozyme-integrated adhesives

Following implantation in the rats, the adhesives with lysozyme (irradiated and non-irradiated) had a significant increase in mass loss from ~7% to ~21% (two-way ANOVA, Bonferroni post-test, $p < 0.001$) over a period of 4 weeks (Fig. 6). In contrast, adhesives free of lysozyme (non-irradiated and irradiated) did not depolmerize significantly after 1 and 4 weeks (~5% and ~8%, respectively, two-way ANOVA, Bonferroni post-test, $p > 0.05$). The *in vitro* and *in vivo* depolymerization of RB–chitosan films containing 1 mg/mL of lysozyme showed comparable mass losses over the treatment period. In agreement with the *in vitro* depolymerization results, the laser did not affect the depolymerization activity of the lysozyme since no significant difference was observed in the mass loss between radiated and non-irradiated samples at 1 or 4 weeks (two-way ANOVA, Bonferroni post-test, $p > 0.05$).

3.5. Scanning electron microscopy

Following removal from the rat, the surface of chitosan films with and without lysozyme (irradiated and non-irradiated) was imaged using SEM to investigate any morphological changes due to depolymerization (Fig. 7). The SEM micrograph of the lysozyme free chitosan films at fabrication showed a smooth and even surface topography (see Fig. 7A). Following 4 weeks implantation, these films revealed a surface with more features and holes scattered on the film (see Fig. 7B). In contrast, micrographs of lysozyme containing films displayed a rough surface with numerous holes (Fig. 7C),

the size of which enlarged at 4 weeks implantation (Fig. 7D). These changes in surface morphologies are in agreement with the *in vitro* and *in vivo* depolymerization profiles, confirming that incorporation of lysozyme in the films enhances the depolymerization rate and prolongs the activity life of the enzyme.

4. Discussion

Suturing tissue is the standard surgical repair technique adopted by surgeons in operating theatres. However, sutures have several disadvantages including foreign body reactions, incomplete tissue sealing and tissue trauma whilst the surgery is a challenging and time consuming task. In a recent report, severe granulomatous reaction was observed in a patient who had the Achilles' tendon repaired with sutures that were made of a silicone coating and a polyethylene core (Ollivere, Bosman, Bearcroft, & Robinson, 2014). Sutures ability to seal tissue is also limited and leakage from colorectal anastomoses, for example, is a very serious complication that leads to significant mortality (6–22%) (Daams, Luyer, & Lange, 2013). The application of sutures thus results in unavoidable post-operative complications, suggesting the full potential of this repair technique has been reached (Menosky, Beek, & Thomsen, 1995). Any repair method which is comparable whilst being simpler, quicker and free from sutures is advantageous. Our group has recently developed the RB chitosan adhesive, which is bonded to tissue by a green laser and is able to repair tissue without sutures (Lauto et al., 2010). Rat median nerves operated using this adhesive achieved better functional recovery than sutured nerves, 12 weeks post-operatively (Barton et al., 2013a,b).

Having the capability to control and manipulate the depolymerization rate of the RB chitosan adhesives is crucial to allow for a broader clinical application of these adhesives instead of sutures. One simple approach to achieve this goal is by incorporating lysozyme in RB chitosan adhesive films. Lysozyme concentrations fluctuate largely in the body, from 1 mg/mL (Temel et al., 1991) in tears to 10 μg/mL in serum (Currie & Eccles, 1976) and 1 μg/mL or lower in cerebrospinal fluid (Mishra, Batra, Ali, Anupurba, & Das, 2003). In our *in vivo* study, we tested adhesives with the lysozyme concentration found in tears (~1 mg/mL) to ensure significant depolymerization, remaining nonetheless in physiological limits. Several concentrations were examined for the *in vitro* study, which varied from 0.5 to 5 mg/mL. Our study confirms that loading lysozyme within the adhesive significantly increases its depolymerization rate (~25%) over a 4 weeks period, the adhesive being bonded to tissue (bonding strength ~15 kPa, unpublished data). Depolymerization products include monomers and oligomers of glucosamine and *N*-acetyl-glucosamine with a large spectrum of molecular weight that spanned from ~200 Da to 2200 Da, as detected by CE–MS. This is in agreement with a previous study where high-performance liquid chromatography and size-exclusion chromatography (SEC–HPLC) was employed to study chitosan depolymerization due to lysozyme (Mengíbar, Mateos-Aparicio, Miralles, & Heras, 2013). The authors reported the presence of a broad range of depolymerized products with different size distribution (0.2–61 kDa) and degree of acetylation (18–39%). Lysozyme is a muramidase capable of hydrolyzing unspecifically certain chitosans with proper degree of acetylation, colloidal chitin (Muzzarelli, Stanic, & Ramos, 1999), and certain modified water-soluble chitosans (Muzzarelli, 1992).

Chitosan depolymerization compounds are biocompatible and have, in the case of the chito-oligosaccharides, antioxidant properties, being able to scavenge 2,2-diphenyl-1-picrylhydrazyl (DPPH) radicals (Mengíbar et al., 2013). The biocompatibility of chitosan-depolymerized products is supported by other studies where the RB chitosan adhesive was applied *in vivo* to peripheral nerves without causing either significant inflammation or tissue damage, acutely or after 3 months (Barton et al., 2013a,b).

Irradiation with laser did not alter appreciably the enzymatic depolymerization of the adhesive films whether the lysozyme was loaded in the film prior to irradiation or solubilized in PBS, in which the irradiated films were incubated. The lysozyme depolymerization activity was thus not significantly changed by the photo-bleaching of RB upon irradiation as indicated by the comparable mass loss observed to non-irradiated films. CE–MS confirmed that irradiated and non-irradiated adhesives were depolymerized into similar products, suggesting that they possibly depolymerized *via* the same route. In this respect, it can be speculated that chitosan molecules inside the adhesive films were not significantly crosslinked following irradiation. This observation is in agreement with a previous study where similar adhesive films maintained their mechanical properties (*E*-modulus and tensile strength) unchanged after being irradiated by the green laser, suggesting that chitosan molecules did not crosslink (Barton et al., 2014).

Of note is the finding that the lysozyme activity inside the chitosan adhesive film persisted for two weeks in our *in vitro* study while lysozyme half-life in physiological conditions has been previously reported to be ~16 h (Rogers & Rechsteiner, 1988). We observed a similar result in the *in vivo* study where films containing the enzyme exhibited a higher mass loss more than films without lysozyme 4 weeks after subcutaneous implantation. The prolonged activity may be partly ascribed to the slow diffusion of lysozyme from the adhesive: Park, Daeschel, and Zhao (2004) showed that chitosan films loaded with lysozyme (~3.3 mg/mL) exhibited only a partial release (~65%) of the enzyme in PBS after 2 days (Park et al., 2004). Further investigations are required to elucidate the mechanism responsible for the activity longevity of lysozyme when added to chitosan adhesive films.

5. Conclusion

The results herein presented showed that loading lysozyme inside the RB chitosan adhesives is a simple and effective technique to tailor the adhesive depolymerization. Remarkably, the laser irradiation does not alter the enzymatic depolymerization products.

References

Aranaz, I., Mengíbar, M., Harris, R., Paños, I., Miralles, B., Acosta, N., et al. (2009). Functional characterization of chitin and chitosan. *Current Chemical Biology*, *3*, 203–230.

Azevedo, H. S., & Reis, R. L. (2007). Understanding the enzymatic degradation of biodegradable polymers and strategies to control their depolymerization rate. In R. L. Reis, & J. San Román (Eds.), *Biodegradable systems in tissue engineering and regenerative medicine* (pp. 177–201). Florida: CRC Press.

Barton, M., Piller, S. C., Mahns, D. A., Morley, J. W., Mawad, D., Longo, L., et al. (2012). In vitro cell compatibility study of rose bengal–chitosan adhesives. *Lasers in Surgery and Medicine*, *44*, 762–768.

Barton, M., Morley, J. W., Stoodley, M. A., Ng, K. S., Piller, S. C., Duong, H., et al. (2013a). Laser-activated adhesive films for sutureless median nerve anastomosis. *Journal of Biophotonics*, *6*, 938–949.

Barton, M. J., Morley, J. W., Stoodley, M. A., Shaikh, S., Mahns, D. A., & Lauto, A. (2013b). Long term recovery of median nerve repair using laser-activated chitosan adhesive films. *Journal of Biophotonics*, http://dx.doi.org/10.1002/jbio.201300129

Barton, M. J., Morley, J. W., Mahns, D. A., Mawad, D., Wuhrer, R., Fania, D., et al. (2014). Tissue repair strength using chitosan adhesives with different physical-chemical characteristics. *Journal of Biophotonics*, http://dx.doi.org/10.1002/jbio.201300148

Costa-Pinto, A. R., Martins, A. M., Castelhano-Carlos, M. J., Correlo, V. M., Sol, P. C., Longatto-Filho, A., et al. (2014). In vitro depolymerization and in vivo biocompatibility of chitosan–poly(butylene succinate) fiber mesh scaffolds. *Journal of Bioactive and Compatible Polymers*, *29*, 137–151.

Cottet, H., & Gareil, P. (2000). From small charged molecules to oligomers: A semiempirical approach to the modeling of actual mobility in free solution. *Electrophoresis*, *21*, 1493–1504.

Currie, G. A., & Eccles, S. A. (1976). Serum lysozyme as a marker of host resistance I. Production by macrophages resident in rat sarcomata. *British Journal of Cancer*, *33*, 51–59.

Daams, F., Luyer, M., & Lange, J. F. (2013). Colorectal anastomotic leakage: Aspects of prevention, detection and treatment. *The World Journal of Gastroenterology*, *19*, 2293–2297.

Kean, T., & Thanou, M. (2010). Biodepolymerization, biodistribution and toxicity of chitosan. *Advanced Drug Delivery Reviews*, *62*, 3–11.

Kim, H., Tator, C. H., & Shoichet, M. S. (2011). Chitosan implants in the rat spinal cord: Biocompatibility and biodepolymerization. *Journal of Biomedical Materials Research, A*, *97A*, 395–404.

Kim, I. Y., Seo, S. J., Moon, H. S., Yoo, M. K., Park, I. Y., Kim, B. C., et al. (2008). Chitosan and its derivatives for tissue engineering applications. *Biotechnology Advances*, *26*, 1–21 [10].

Kochevar, I. E., & Redmond, R. W. (2000). Photosensitized production of singlet oxygen. *Methods in Enzymology*, *319*, 20–28.

Lauto, A., Mawad, D., Barton, M., Gupta, A., Piller, S. C., & Hook, J. (2010). Photochemical tissue bonding with chitosan adhesive film. *Biomedical Engineering Online*, *9*, 47.

Lauto, A., Stoodley, M., Barton, M., Morley, J., Mahns, D., Longo, L., et al. (2012). Fabrication and application of rose-bengal–chitosan films in laser tissue repair. *Journal of Visual Experiments*, *68*, e4158. http://dx.doi.org/10.3791/4158

Mengíbar, M., Mateos-Aparicio, I., Miralles, B., & Heras, A. (2013). Influence of the physico-chemical characteristics of chito-oligosaccharides (COS) on antioxidant activity. *Carbohydrate Polymers*, *97*, 776–782.

Menovsky, T., Beek, J. F., & Thomsen, S. L. (1995). Laser (assisted) nerve repair: A review. *Neurosurgery Reviews*, *18*, 225–235.

Mi, F., Tan, Y., Liang, H., & Sung, H. (2002). In vivo biocompatibility and degradability of a novel injectable-chitosan-based implant. *Biomaterials*, *23*, 181–191.

Mishra, O. P., Batra, P., Ali, Z., Anupurba, S., & Das, B. K. (2003). Cerebrospinal fluid lysozyme level for the diagnosis of tuberculous meningitis in children. *Journal of Tropical Paediatrics*, *49*, 13–16.

Mnatsakanyan, M., Thevarajah, J. J., Roi, R. S., Lauto, A., Gaborieau, M., & Castignolles, P. (2013). Separation of chitosan by degree of acetylation using simple free solution capillary electrophoresis. *Analytical and Bioanalytical Chemistry*, *405*, 6873–6877.

Muzzarelli, R. A. A. (1992). Depolymerization of methyl pyrrolidinone chitosan by lysozyme. *Carbohydrate Polymers*, *19*, 29–34.

Muzzarelli, R. A. A., Stanic, V., & Ramos, V. (1999). Enzymatic depolymerization of chitins and chitosans. In C. Bucke (Ed.), *Methods in biotechnology: Carbohydrate biotechnology protocols*. Totowa, NJ: Humana Press.

Muzzarelli, R. A. A. (2009). Chitins and chitosans for the repair of wounded skin, nerve, cartilage and bone. *Carbohydrate Polymers*, *76*, 167–182.

Obara, K., Ishihara, M., Ishizuka, T., Fujita, M., Ozeki, Y., Maehara, T., et al. (2003). Photocrosslinkable chitosan hydrogel containing fibroblast growth factor-2 stimulates wound healing in healing-impaired db/db mice. *Biomaterials*, *24*, 3437–3444.

Ollivere, B. J., Bosman, H. A., Bearcroft, P. W., & Robinson, A. H. (2014). Foreign body granulomatous reaction associated with polyethelene 'Fiberwire(®)' suture material used in Achilles tendon repair. *Foot and Ankle Surgery*, *5*, 720–722.

Park, S. I., Daeschel, M. A., & Zhao, Y. (2004). Functional properties of antimicrobial lysozyme-chitosan composite films. *Journal of Food Science*, *69*, M215–M221.

Rogers, S. W., & Rechsteiner, M. (1988). Depolymerization of structurally characterized proteins injected into HeLa cells. Basic measurements. *The Journal of Biological Chemistry*, *263*, 19833–19842.

Sionkowska, A. (2011). Current research on the blends of natural and synthetic polymers as new biomaterials: Review. *Progress in Polymer Science*, *36*, 1254–1276.

Temel, A., Kazokoglu, H., & Taga, Y. (1991). Tear lysozyme levels in contact lens wearers. *Annals of Ophthalmology*, *23*, 191–194.

Verter, E. E., Gisel, T. E., Yang, P., Johnson, A. J., Redmond, R. W., & Kochevar, I. E. (2011). Light-initiated bonding of amniotic membrane to cornea. *Investigative Ophthalmology and Visual Science*, *52*, 9470–9477.

Warren, C. R. (2013). Development of a capillary electrophoresis–mass spectrometry method for small peptides in the soil solution. *Soil Biology and Biochemistry*, *63*, 80–84.

Zhao, H., Wang, K., Zhao, Y., & Pan, L. (2002). Novel sustained-release implant of herb extract using chitosan. *Biomaterials*, *23*, 4459–4462.